Comparisons among computed tomographic features of adipose masses in dogs and cats

COMPARISONS AMONG COMPUTED TOMOGRAPHIC FEATURES OF ADIPOSE MASSES IN DOGS AND CATS

ELISA SPOLDI, TOBIAS SCHWARZ, SILVIA SABATTINI, MASSIMO VIGNOLI, SIMONA CANCEDDA, FEDERICA ROSSI

A better understanding of the CT features of different forms of canine and feline adipose tumors would be valuable for improving patient management and treatment. The purpose of this retrospective, cross-sectional study was to describe and compare the CT features of pathologically confirmed lipomas, infiltrative lipomas, and liposarcomas in a sample of canine and feline patients. A total of 50 animals (46 dogs, four cats) and a total of 60 lesions (23 lipomas, 20 infiltrative lipomas, and 17 liposarcomas) were included in the study. Lipomas appeared as round to oval-shaped ($n = 21$), well-marginated ($n = 20$) fat-attenuating lesions. Infiltrative lipomas appeared as homogeneous, fat-attenuating masses but, unlike lipomas, they were most commonly characterized by an irregular shape (75%; $P < 0.001$), and linear components, hyperattenuating relative to the surrounding fat (100%; $P < 0.05$). Liposarcomas were represented exclusively by heterogeneous lesions with soft tissue attenuating components with a multinodular appearance (76.5%; $P < 0.05$). Regional lymphadenopathy ($n = 10$) and amorphous mineralization ($n = 4$) were also observed in association with liposarcomas. Computed tomography can provide useful information regarding disease location, extent, and involvement of the adjacent structures. Tumor definition and shape were the most useful parameters to differentiate between lipomas and infiltrative lipomas. The presence of a heterogeneous mass, with a multinodular soft tissue component and associated regional lymphadenopathy and mineralization, were features favoring a diagnosis of liposarcoma.

Key words: CT, canine, feline, infiltrative lipoma, lipoma, liposarcoma.

Introduction

THE CURRENT WORLD HEALTH ORGANIZATION (WHO) classification of mesenchymal skin and soft tissue tumors of domestic animals recognizes three benign forms of tumors of the adipose tissue, represented by lipoma, infiltrative lipoma and angiolipoma, and one malignant form, represented by liposarcoma.[1] Lipomas are tumors characterized by well-differentiated adipocytes that are common in the dog, with a reported incidence rate of 5.1% of all diagnosed canine neoplasms, while they are far less common in other species.[2,3] Lipomas are defined as infiltrative when they show a more aggressive biological behavior by invading adjacent structures, most commonly muscle and fasciae.[1,4–8] Angiolipoma is another uncommon variant of lipoma characterized by the presence of small, well-differentiated blood vessels interspersed in mature adipose tissue that can be further subclassified as infiltrative or noninfiltrative.[1,9] Liposarcoma, the rare malignant counterpart of lipoma, is histologically characterized by lipoblasts with variable grade of pleomorphism.[1] Liposarcomas have been further classified into subtypes based on cellular morphology, however the different histological appearances do not correspond to differences in biological behavior in domestic animals.[1,3] Although liposarcomas generally show a low metastatic potential, they are characterized by local invasion and high recurrence rate.[1,10–18]

While the majority of lipomas are asymptomatic and do not require surgical intervention, aggressive treatment may be necessary for the local control of infiltrative lipomas and liposarcomas. Therefore, a correct diagnosis is essential for prognosis and therapy planning. Infiltrative lipomas cannot be readily distinguished from simple lipomas in fine

From the Small Animal Clinical Sciences, University of Florida College of Veterinary Medicine, Gainesville, FL 32610 (Spoldi), Royal (Dick) School of Veterinary Studies, Easter Bush Veterinary Centre, University of Edinburgh, Roslin, Midlothian, Scotland, UK (Schwarz), the Department of Veterinary Medical Sciences, University of Bologna, Ozzano Emilia, Bologna, Italy (Sabattini), Universita degli Studi di Teramo Facolta di Medicina Veterinaria, Teramo, Abruzzo, Italy (Vignoli), Centro Oncologico Veterinario, Sasso Marconi, Italy (Cancedda), and Clinica Veterinaria dell'Orologio, Sasso Marconi, Bologna, Italy (Rossi).

Previous abstract: E. Spoldi, T. Schwarz, M. Vignoli, S. Cancedda, F. Rossi. Computed tomographic features of canine and feline adipous masses. 2013 ECVDI and EAVDI Annual Meeting, Cascais, Portugal: Vet Rad & Ultrasound, Vol. 55, No. 6, 651–679.
Portions of this study were presented at the 2013 ECVDI and EAVDI Annual Meeting, Cascais, Portugal.

Address correspondence and reprint requests to Elisa Spoldi, at the above address. E-mail: espoldi@ufl.edu

Received February 14, 2016; accepted for publication September 26, 2016.
doi: 10.1111/vru.12445

needle aspirates or small biopsy specimens.[17] Computed tomography is currently used to better delineate these tumors, evaluate their actual extension and assess their relationship with the adjacent anatomic structures, allowing for accurate treatment planning.[7,19–27]

The CT and MRI appearance of fat-containing tumors has previously been described in humans. Both modalities have been proven to be useful in identifying and characterizing adipose masses.[28–42] In veterinary medicine there are a few reports describing adipose tumors, but there is only limited information available on their CT features.[7,19–27,43] Moreover, a comparison between benign and malignant fatty masses based on CT characteristics in a larger group of animals has not been reported. Diagnostic imaging would be a valuable and noninvasive procedure to discriminate between the different neoplastic forms and assess their growth pattern before treatment planning.[3,19,44,45] The aim of this study was to describe and compare CT features of histologically confirmed lipomas, infiltrative lipomas, and liposarcomas in dogs and cats.

Material and Methods

The study was a retrospective, cross-sectional design. Patients were selected from two board-certified veterinary radiologist (T.S., F.R.) on the basis of having helical CT evaluation and a confirmed histological diagnosis of lipoma, infiltrative lipoma, or liposarcoma. Cases were retrieved from the electronic database of the Clinica Veterinaria dell'Orologio and the Royal (Dick) School of Veterinary Studies, University of Edinburgh, and chosen from clinical databases from January 2005 through June 2015. Images were acquired using one of the following three different CT scanners: helical single-slice CT unit (ProSpeed, GE, Milwaukee), helical 4-slice CT unit (Somatom Volume Zoom, Siemens, Germany) and helical 16-slice CT unit (BrightSpeed, GE, Milwaukee). All CT studies were performed under general anesthesia. To ensure the greatest consistency in evaluation of imaging features, the images were retrospectively reviewed and reevaluated in a randomized order by the primary author (E.S.) and one board-certified veterinary radiologist (F.R.), who were unaware of the final diagnosis at the time of the image review. Images measurements were made in triplicate by each reviewer and final assessment was reached by means of consensus. Images were reviewed following determination of the computed tomographic characteristics by using image analysis freeware (OsiriX v.4.1.2 32-bit, Pixmeo Sàrl, Geneva, Switzerland). Display settings were adjusted as needed for optimal evaluation of the images.

CT images were reviewed and assessed for the following criteria:

1. Volume of the mass was measured by the rotational ellipse method: the largest tumor diameter was measured in the three orthogonal planes on CT images and volume was calculated as the product of the three measurements times $\pi/6$.
2. Shape of the mass: defined as round to oval or irregular (for all the lesions that were neither round nor oval in shape).
3. Tumor definition: margins were classified on the postcontrast series as well-defined (presence of a distinct border to surrounding tissues), poorly defined (absence of a distinct border to surrounding tissues), or a combination of well-defined and poorly defined regions.
4. Pre- and postcontrast homogeneity and attenuation characteristics of the lesion were evaluated subjectively and by measuring Hounsfield Unit (HU) values. Overall lesion attenuation was calculated by placing different regions of interest (ROIs) on pre- and postcontrast series. The mean HU values were recorded for the different series.
5. Prevalence of a fat or a soft tissue component was evaluated based on the HU values.
6. Presence of intralesional areas that are hyperattenuating compared to fat (defined as hyperattenuating components).
7. Type of hyperattenuating component classified as linear (presence of hyperattenuating septa) or as nodular-globular-mass (presence of irregular conglomerate areas).
8. Presence of mineral attenuating areas within the lesion.
9. Presence of regional lymphadenopathy (round, enlarged, and/or heterogeneously contrast enhancing lymph nodes). Normal lymph nodes are oval in shape, smoothly marginated with a uniform appearance and are soft tissue attenuating.
10. Evidence of potential metastatic lesions (round, enlarged, irregularly marginated and/or heterogeneous, heterogeneously contrast enhancing lymph nodes or other nodules/masses distant from the primary lesion).

None of the masses underwent cytoreductive surgery or incisional biopsy prior to imaging. Definitive diagnoses were based on histopathological examination of surgical or postmortem specimens, according to the WHO criteria.[1] The samples were not available for review or for mapping correlation with the CT images.

Data were analyzed with commercial software programs (SPSS Statistics v. 19, IBM, Somers, NY, and Prism v. 5.0, GraphPad, San Diego, CA) by one of the authors (SS, DVM, PhD in animal pathology and biotechnology). When appropriate, data sets were tested for normality by using the D'Agostino and Pearson omnibus normality test. Values were expressed as mean ± standard deviation for normal distribution, or as median with a range for nonnormal distribution. Differences in the

TABLE 1. Summary of Signalment for Each Tumor Type Group (Lipoma, Infiltrative Lipoma, and Liposarcoma)

	Lipoma ($n = 18$)	Infiltrative lipoma ($n = 18$)	Liposarcoma ($n = 15$)
Species, breed			
Dogs	15	17	15
Labrador retriever	5	6	1
Weimaraner	0	0	2
Other breeds	4*	5†	6‡
Mongrel	6	6	6
Cats	3	1	0
Persian	2	0	0
Domestic shorthair	1	1	0
Gender			
Male	3 (1 castrated)	11 (3 castrated)	12 (1 castrated)
Female	15 (3 spayed)	7 (1 spayed)	3 (0 spayed)
Age			
Median (range)	11 years (1–13)	8.8 years (3–15)	10.5 years (2–14)

Numbers indicate number of patients.
*Other breeds include a single patient representing each of the following breeds: English Setter, Border Collie, Doberman Pinscher, Bernese Mountain Dog.
†Other breeds include a single patient representing each of the following breeds: Chihuahua, English Springer Spaniel, Shih Tzu, Dachshund, Siberian Husky.
‡Other breeds include a single patient representing each of the following breeds: Samoyed, West Highland White Terrier, Rottweiler, German Shepherd Dog, Doberman Pinscher, Bearded Collie.

TABLE 2. CT Features within Benign Adipose Masses

Parameters	Lipoma ($n = 23$)	Infiltrative Lipoma ($n = 20$)	Significance (P value)*
Volume median	115.7 cm^3	157.9 cm^3	0.342
(Range)	(1.6–1457.0)	(0.1–5073.7)	
Shape			<0.001
Oval/round	21 (91.3%)	5 (25%)	
Irregular	2 (8.7%)	15 (75%)	
Margins			0.005
Well-defined	20 (87%)	9 (45%)	
Mixed	3 (13%)	8 (40%)	
Poorly-defined	0 (0%)	3 (15%)	
Attenuation			0.6
Homogeneous	18 (78.3%)	16 (80%)	
Heterogeneous	5 (21.7%)	4 (20%)	
Precontrast attenuation			0.8
Median	−120.0 HU	−113.0 HU	
(Range)	(−130.0 to −6.0)	(−134.0 to −23.0)	
Postcontrast attenuation			0.7
Median	−113.5 HU	−103.5 HU	
(Range)	(−157.0–27.0)	(−133.0 to −18.0)	
Prevalent component			1
Fat	23 (100%)	20 (100%)	
Soft tissue	0 (0%)	0 (0%)	
Hyperattenuating components	10 (43.5%)	17 (85%)	0.01
Type of hyperattenuating component†			0.04
Linear	7 (70%)	17 (100%)	
Nodular/globular/mass	3 (30%)	0 (0%)	
Mineralization	0 (0%)	0 (0%)	1
Regional lymphadenopathy	4 (17.4%)	5 (25%)	0.711
Metastatic lesions	0 (0%)	0 (0%)	1

Numbers indicate number of lesions.
*Continuous variables compared by using Mann–Whitney U test, categorical variables compared by using Chi Square test/Fisher's exact test.
†Percentages are calculated for each group on the total number of masses showing hyperattenuating components.

demographic and CT parameters between lipomas and liposarcomas and between infiltrative and noninfiltrative lipomas were evaluated with Mann–Whitney U test (continuous variables) and Chi Square/Fisher's exact test (categorical variables). Binary logistic regression model was performed to estimate which study variables best-predicted tumor type. For all analyses, P values of ≤ 0.05 were considered significant.

Results

A total of 50 patients met the inclusion criteria ($n = 46$ dogs; $n = 4$ cats). None of the total number of patients with a helical CT evaluation and a confirmed histological diagnosis of lipoma, infiltrative lipoma or liposarcoma were excluded from the data analysis. Signalment characteristics of animals for each tumor type are summarized in Table 1. Eight dogs had two lesions and one dog had three lesions, for a total of 60 lesions. Definitive diagnoses included 23 lipomas (15 dogs and three cats), 20 infiltrative lipomas (17 dogs and one cat), and 17 liposarcomas (15 dogs). Only one dog had both a lipoma and an infiltrative lipoma. None of the cases were diagnosed as angiolipoma or infiltrative angiolipoma. Ten tumors were intracavitary (thorax or abdomen) and included four lipomas, four infiltrative lipomas, and two liposarcomas. The extracavitary neoplasms included four lesions within the head-neck region (two lipomas, one infiltrative lipoma, and one liposarcoma); 14 lesions located in the thoracic or pelvic limbs (five lipomas, eight infiltrative lipomas, and one liposarcoma); and 32 lesions located within the trunk (12 lipomas, seven infiltrative lipomas, and 13 liposarcomas).

Helical CT scans of the whole body ($n = 34$) or of the area of interest ($n = 16$) were acquired before and after intravenous administration of a bolus of water-soluble contrast medium (Ioversol 300 mgI/ml Optiray, Covidien, Segrate, Italy; Iopramide 370 mgI/ml, Ultravist 370, Bayer, Germany) at a dose of 600 or 740 mg Iodine/kg with the use of a power injector or manual injection. Only precontrast images were available for five lesions and only postcontrast images were available for three other lesions. Tube voltage was consistent at 120 kVp, adaptive tube current ranged from 127 to 220 mAs, tube rotation time was between 0.5 and 1.5 s, slice thickness varied from 1 to 7 mm, image interval ranged from 0.625 to 7 mm, helical collimator pitch from 0.625 to 1.75, display field of view from 242 to 354 mm-based on patient size, body part imaged, and

TABLE 3. CT Features of Benign Versus Malignant Adipose Masses

Parameters	Lipoma and infiltrative lipoma ($n = 43$)	Liposarcoma ($n = 17$)	Significance (P value)*
Volume median	115.7 cm^3	175.9 cm^3	0.583
(Range)	(0.1–5073.7)	(4.6–3225.4)	
Shape			0.1
Oval/round	26 (60.5%)	14 (82.3%)	
Irregular	17 (39.5%)	3 (17.4%)	
Margins			0.6
Well-defined	29 (67.4%)	9 (53%)	
Mixed	11 (25.6%)	6 (35.3%)	
Poorly-defined	3 (7%)	2 (11.7%)	
Attenuation			<0.001
Homogeneous	34 (79.1%)	0 (0%)	
Heterogeneous	9 (20.9%)	17 (100%)	
Precontrast attenuation			<0.001
Median	−113.0 HU	−5 HU	
(Range)	(−134.0 to -6.0)	(−49.0 to 28.0)	
Postcontrast attenuation			<0.001
Median	−111.0 HU	13.0 HU	
(Range)	(−157.0 to 27.0)	(−48.0 to 61.0)	
Prevalent component			<0.001
Fat	43 (100%)	9 (52.9%)	
Soft tissue	0 (0%)	8 (47%)	
Hyperattenuating components	27 (62.8%)	17 (100%)	0.003
Type of hyperattenuating component†			<0.001
Linear	24 (88.9%)	4 (23.5%)	
Nodular/globular/mass	3 (11.1%)	13 (76.5%)	
Mineralization	0 (0%)	4 (23.5%)	0.005
Regional lymphadenopathy	9 (20.9%)	10 (58.8%)	0.007
Metastatic lesions	0 (0%)	1 (5.9%)	0.3

Numbers indicate number of lesions.
*Continuous variables compared by using Mann–Whitney U test, categorical variables compared by using Chi Square test/Fisher's Exact test.
†Percentages are calculated for each group on the total number of masses showing hyperattenuating components.

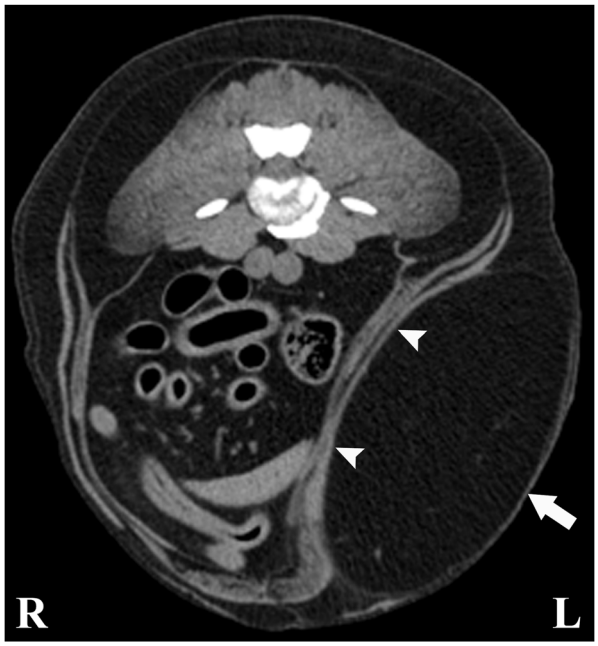

FIG. 1. Transverse image of an 11-year old intact female Labrador Retriever diagnosed with a lipoma. At the level of the sixth lumbar vertebra, there is a large, oval shaped, homogeneously fat attenuating mass (white arrow), compressing the adjacent abdominal wall (white arrowheads) and axially displacing the intrabdominal organs at that level. No infiltration of the adjacent abdominal wall is detected. Window width (WW) = 400, Window level (WL) = 40.

radiologist preference. The protocols included two reconstruction algorithms, medium frequency for soft tissue and high frequency for lung. Patient positioning was sternal ($n = 45$) or dorsal ($n = 5$) recumbency. In one patient, two different body regions were evaluated with two different studies, one with the dog in dorsal recumbency and the following with the dog in sternal recumbency. The CT findings for each tumor type are summarized in Tables 2 and 3.

Lipomas were round- to oval-shaped ($n = 21$, 91.3%), with well-defined margins ($n = 20$, 87%) and homogeneously attenuating ($n = 18$, 78.3%) (Fig. 1). In all cases there was prevalent fat attenuation ($n = 23$, 100%), with a median precontrast attenuation of –120 HU (range = –130 to –6 HU) and a median postcontrast attenuation of –113.5 HU (range = –157 to 27 HU). However, presence of hyperattenuating components, linear ($n = 7$, 70%) or irregular conglomerate areas ($n = 3$, 30%), was identified in 10 cases (43.5%) (Fig. 2). Regional lymphadenopathy was seen in four cases (17.4%).

Infiltrative lipomas appeared irregular in shape ($n = 15$, 75%), with well- ($n = 9$, 45%), mixed- ($n = 8$, 40%), or poorly-demarcated margin definition ($n = 3$, 15%). Masses were homogeneous ($n = 16$, 80%), with prevalent fat attenuation in all cases ($n = 20$, 100%), with a median precontrast attenuation of −113 HU (range = −134 to −23 HU) and postcontrast of −103.5 HU (range −133 to −18 HU). In seventeen cases (85%) hyperattenuating components were seen, but were all linear in appearance (Fig. 3). Regional lymphadenopathy was present in five cases (25%). CT parameters significantly different between lipomas and infiltrative lipomas included shape ($P < 0.001$), margins ($P = 0.005$), presence and type of hyperattenuating components ($P = 0.01$ and $P = 0.04$, respectively; Table 2).

A high percentage of liposarcomas ($n = 14$; 82.3%) were round to oval shaped. Margins were well- ($n = 9$, 53%), mixed- ($n = 6$, 35.3%) or poorly-defined ($n = 2$, 11.7%). All the lesions were heterogeneous with hyperattenuating components, mostly represented by nodular-globular-mass-like conglomerates ($n = 13$, 76.5%). Median attenuation values varied from –5 HU precontrast (range = –49 to 28) to 13 HU postcontrast (range = –48 to 61). In four cases amorphous mineralized areas were observed. Two lesions determined osteolysis of the adjacent skeletal structures (Fig. 4). Regional lymphadenopathy was observed

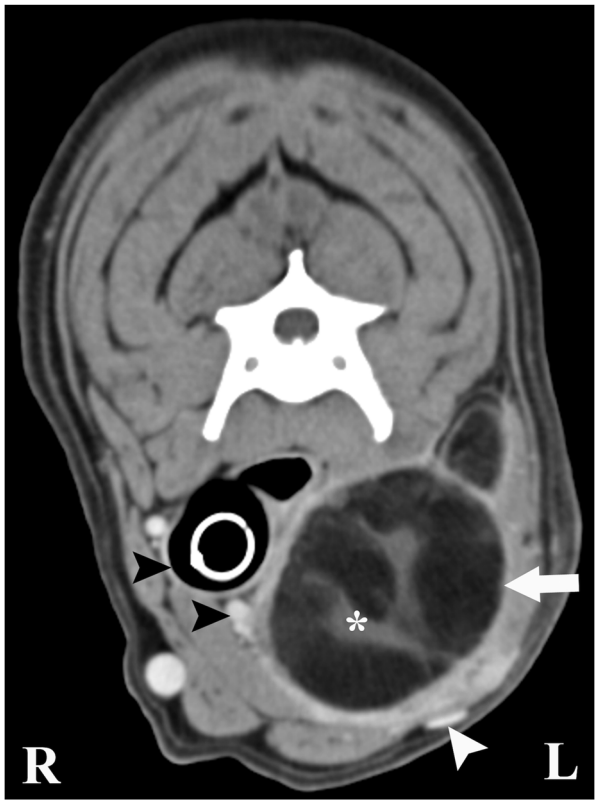

FIG. 2. Transverse contrast-enhanced image of an 11-year old neutered male mongrel diagnosed with a necrotic lipoma. At the level of the fourth cervical vertebra, there is a heterogeneously predominately fat attenuating mass (white arrow) with hyperattenuating striations (white asterisk) revealed histopathologically as necrotic, inflamed fat interposed within the mass. The mass is displacing the trachea, left carotid artery, and sympathetic trunk rightwards (black arrowheads). The left jugular vein is compressed by this mass (white arrowhead). WW = 400, WL = 40.

FIG. 3. Dorsal contrast-enhanced image of a 5-year old neutered male Springer Spaniel diagnosed with an infiltrative lipoma. At the level of the left axillary region and cranial thoracic wall, there is an oval shaped, noncontrast medium enhancing, homogeneously fat attenuating mass (white arrow) with a combination of well-defined and ill-defined margins characterized by fine wispy linear striations throughout (white asterisks). Medially the mass extends and infiltrates through the musculature of the thoracic inlet and cranial thoracic wall (white arrowheads) and contacts the left first and second ribs without evidence of osteolysis. The linear hyperattenuating striations represent the residual muscular components of the pectoralis and serratus ventralis muscles. WW = 700, WL = 150.

in 10 cases (58.8%). A suspected metastatic lesion was seen in one case (Fig. 5). Computed tomographic features significantly different between benign (lipoma/infiltrative lipoma) and malignant forms were pre- and postcontrast homogeneity ($P < 0.001$), attenuation characteristics ($P < 0.001$), prevalent component ($P < 0.001$); presence and type of hyperattenuating components ($P < 0.001$ and $P = 0.003$, respectively), mineralization ($P = 0.005$), and regional lymphadenopathy ($P = 0.007$; Table 3). On logistic regression, presence of a heterogeneous lesion, with a prevailing soft tissue component showing an irregular conglomerate appearance, together with the presence of mineralization and regional lymphadenopathy were features with statistically significant odds ratio favoring a diagnosis of a malignant form (Table 4). Presence of well-defined lesions without any evidence of hyperattenuating component within the mass, and presence of an irregularly shaped mass are features with statistically significant odds ratio favoring a diagnosis of lipoma and infiltrating lipoma, respectively (Table 4).

Discussion

This retrospective study described CT features of adipose masses that warrant a higher suspicion for infiltration and malignancy. In the current study, none of the masses underwent cytoreductive surgery or incisional biopsy prior to imaging and all adipose masses showed complete or partial fat attenuation. The majority of the benign tumors in this study appeared as a homogenous mass while liposarcomas were all represented by heterogenous masses with a large component of nonadipose tissue, generally characterized by a more nodular appearance, consistent with the literature.[37,40] Nevertheless, as previously reported, a high percentage of the benign forms identified in this study showed a heterogeneous appearance, with presence of hyperattenuation components within.[22,37,39,46,47] The exact cause of these characteristics remains unknown because the pathologic samples were not available for review or for mapping correlation with the CT images. According to the literature and the pathologic reports available, the authors propose that these regions most likely represented areas of

FIG. 4. Transverse image of an 11-year old intact male Rottweiler diagnosed with a liposarcoma. There is an oval shaped, heterogeneous mass with well-demarcated (white arrowheads) as well as poorly demarcated (white arrows) margins, causing lysis of the left iliac wing and left transverse process of the seventh lumbar vertebra (black arrowheads). This mass has a soft tissue component with a nodular appearance centrally (white asterisk). WW = 700, WL = 150.

TABLE 4. Features Favoring a Diagnosis of Liposarcoma, Lipoma, and Infiltrative Lipoma

Features	Odds ratio	95% CI	*P* value
Liposarcoma			
Heterogeneous attenuation	60.4	7.0–518.8	< 0.001
Prevalence of soft tissue component	37.3	4.1–336.9	0.001
Nodular/globular/mass hyperattenuating component	26.0	5.0–134.3	< 0.001
Mineralization	12.9	1.3–126.1	0.03
Regional lymphadenopathy	5.4	1.6–18.2	0.006
Lipoma			
Well-defined margins	7.0	1.8–27.8	0.005
Absence of hyperattenuating component	14.7	3.5–62.2	< 0.001
Infiltrative lipoma			
Irregular shape	21.0	5.3–83.4	< 0.001

necrosis/hemorrhage or fibrosis in lipomas, and residual muscular bands in the infiltrative lipomas.[31,32,34,37,38]

The current study also reported odds ratios to help distinguish between the different forms of fat-containing tumors. These demonstrated that the most useful features to help distinguish between benign and malignant forms were the presence of a heterogeneous mass, with prevailing soft tissue component characterized by multinodular appearance and possible presence of mineral attenuating areas within, and associated with regional lymphadenopathy. In agreement with previous reports, the irregular shape was the most significant parameter favoring a diagnosis of infiltrating lipoma.[20,41,44] The most helpful features in recognizing lipoma were the presence of a well-defined mass without associated hyperattenuating components. In general, the fat attenuating lesions did not show contrast-medium enhancement, except for some peripheral areas in those masses characterized by a fibrous capsule or perilesional inflammation, consistent with previous reported data.[20–22,24,27,37,38,48] Evidence of bone involvement has been reported in patients with infiltrative lipomas.[6,49] In this study, only three cases of liposarcomas showed an involvement of skeletal structures adjacent to the neoplastic lesion.

There were several limitations in this study. Firstly, this was a retrospective study, so no standardized protocols were established and only precontrast studies were available for five lesions and only postcontrast studies were available for three lesions. Also, there were a limited number of cases. In particular, the number of feline patients to feline masses was extremely small. Only the excised large lipomas causing clinical abnormalities for either compression or location were included in the study since the availability of the histopathology represented one of the inclusion criteria. The entire spectrum of adipose masses was not represented in our sample. In fact we did not have any cases of angiolipoma or infiltrating angiolipoma. The absence of cytologic confirmation and characterization of the regional lymphadenopathy and potential metastatic lesion was another limitation of the current study. Also, as previously mentioned, the pathological specimens were not available for review, thus a mapping correlation between the CT and the histopathological images was not possible.

In conclusion, findings supported the use of CT as a modality for assessing adipose tumor location, shape, extension, and relationship with the adjacent anatomic structures in dogs and cats. Although some CT features were shared by the different groups of fat-containing tumors, the present study identified several statistically significant features such as attenuation characteristics, margins, shape, and presence of regional lymphadenopathy, that are helpful to distinguish between adipose masses. Nevertheless, histopathology will be required to obtain a definitive diagnosis. Additional prospective studies comparing CT findings and gross pathological lesion patterns are needed to further characterize CT features of malignancy for fat-containing tumors.

LIST OF AUTHOR CONTRIBUTIONS

Category 1

(a) Conception and Design: Elisa Spoldi, Tobias Schwarz, Silvia Sabattini, Federica Rossi

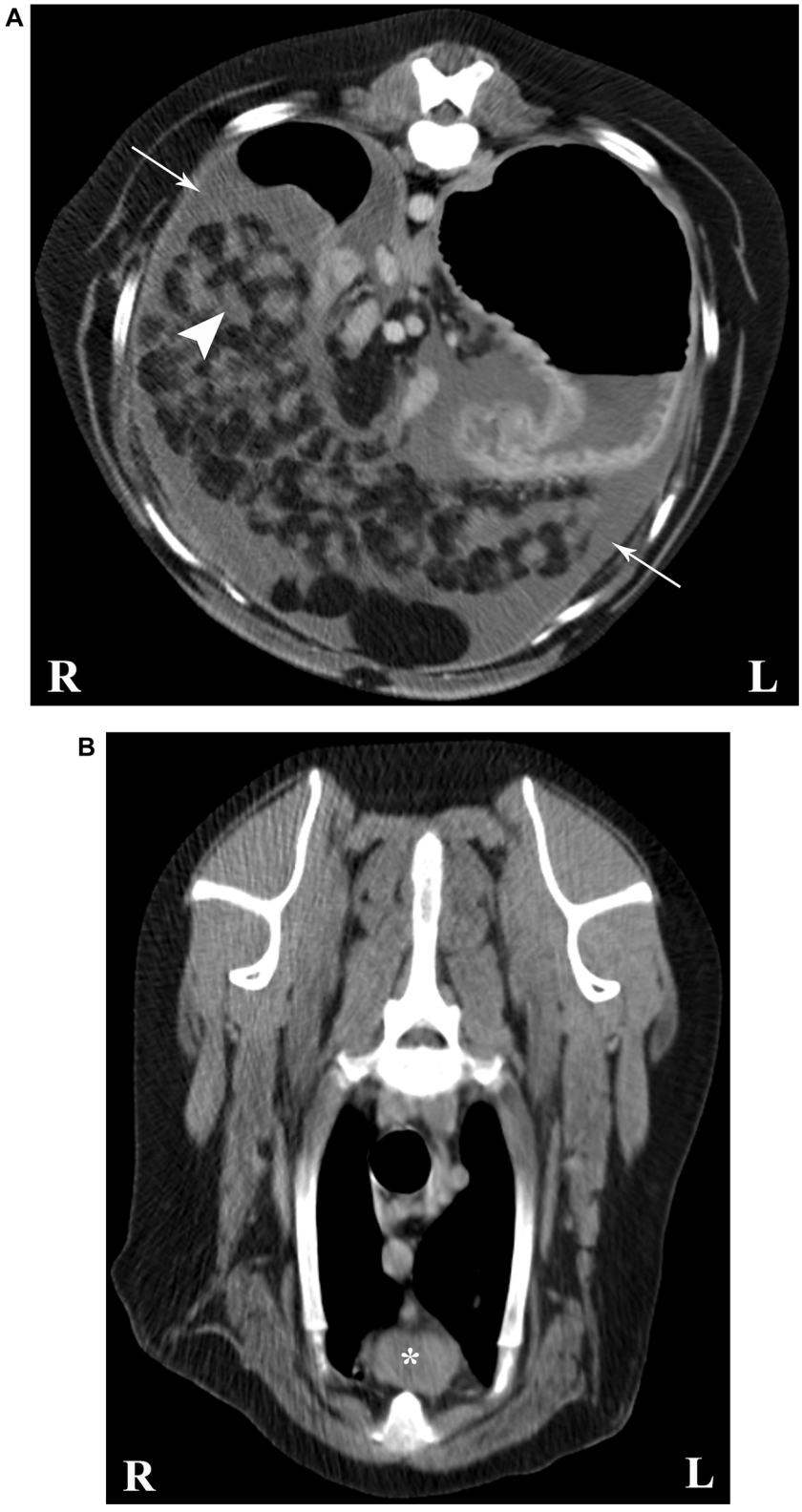

FIG. 5. Transverse contrast-enhanced image at the level of the stomach (A) in an 8-year-old intact female German Shepherd diagnosed with a liposarcoma. There is a multifocal to coalescing, predominantly heterogeneously fat attenuating mass with irregular nodular soft tissue component (white arrowhead) within the peritoneal cavity. There is a large amount of gravity-dependent abdominal fluid (white arrows). WW = 400, WL = 40.

Transverse contrast enhanced image in the same patient diagnosed with an intrabdominal liposarcoma (B). The sternal lymph node (white asterisk) is severely enlarged with rounded, lobulated margins, and heterogeneous contrast enhancement. WW = 400, WL = 40.

(b) Acquisition of Data: Elisa Spoldi, Tobias Schwarz, Massimo Vignoli, Simona Cancedda, Federica Rossi
(c) Analysis and Interpretation of Data: Elisa Spoldi, Silvia Sabattini, Federica Rossi

Category 2

(a) Drafting the Article: Elisa Spoldi

(b) Revising the Article for Intellectual Content: Elisa Spoldi, Tobias Schwarz, Silvia Sabattini, Massimo Vignoli, Simona Cancedda, Federica Rossi

Category 3

(a) Final Approval for the Completed Article: Elisa Spoldi, Tobias Schwarz, Silvia Sabattini, Massimo Vignoli, Simona Cancedda, Federica Rossi

REFERENCES

1. Hendrick MJ. Tumors of adipose tissue. In: Hendrick MJ (ed): Histological classification of mesenchymal tumors of skin and soft tissues of domestic animals. Washington, DC.: Armed Forces Institute of Pathology in cooperation with the American Registry of Pathology and the World Health Organization Collaborating Center for Worldwide Reference on Comparative Oncology, 1998;11–60.
2. Strafuss AC, Smith JE, Kennedy GA, Dennis SM. Lipomas in dogs. J Am Anim Hosp Assoc 1973;9:555.
3. Goldschmidt MH, Hendrick MJ. Tumors of the skin and soft tissues. In: Meuten DJ (ed): Tumors in domestic animals. Ames, Iowa: Iowa State Press, 2002;96–97.
4. Gleiser CA, Jardine JH, Raulston GL, Gray KN. Infiltrating lipomas in the dog. Vet Pathol 1979;16:623–624.
5. Kramek BA, Spackman JA, Hayden DW. Infiltrative lipoma in three dogs. J Am Vet Med Assoc 1985;186:81–82.
6. Bergman PJ, Withrow SJ, Straw RC, Powers BE. Infiltrative lipoma in dogs: 16 cases (1981–1992). J Am Vet Med Assoc 1994;205:322–324.
7. Bruckner M, Wigger A, Peppler C, Kramer M, Thiel M, Henrich M. Das infiltrative lipom beim hund: eine retrospective studie von funf fallen. Tieraerztl Prax 2009;37:305–313.
8. McChesney AE, Stephens LC, Lebel J, Snyder S, Ferguson HR. Infiltrative lipoma in dogs. Vet Pathol 1980;17:316–322.
9. Liggett AD, Frazier KS, Styer EL. Angiolipomatous tumors in dogs and a cat. Vet Pathol 2002;39:286–289.
10. Bozarth AJ, Strafuss AC. Metastatic liposarcoma in a dog. J Am Vet Med Assoc 1973;162:1043–1044.
11. Davis PE, Dixon RT, Johnson JA, Paris R. Multiple liposarcoma of bone marrow origin in a Greyhound. J Small Anim Pract 1974;15:445–456.
12. Misdorp W, van der Heul RO. An osteo-(chondro-)liposarcoma ("malignant mesenchymoma") of the radius in a dog, with two types of metastases. Zentralbl Veterinarmed A 1975;22:187–192.
13. Saik JE, Diters RW, Wortman JA. Metastasis of a well-differentiated liposarcoma in a dog and a note on nomenclature of fatty tumours. J Comp Pathol 1987;97:369–373.
14. Theilen GH, Madewell BR. Veterinary cancer medicine. Philadelphia: Lea & Febiger, 1987.
15. Chang SC, Liao JW. Mesojejunoileac liposarcoma with intrahepatic metastasis in a dog. J Vet Med Sci 2008;70:637–640.
16. Frase R, Freytag M, Baumgartner W, Wohlsein P. Metastasising liposarcoma of bone in a young dog. Vet Rec 2009;164:372–373.
17. Liptak JM, Forrest LJ. Soft tissue sarcomas. In: Withrow SJ, Vail DM, Page RL (eds): Withrow and MacEwen's small animal clinical oncology. St. Louis: Saunders Elsevier, 2013;356–380.
18. Baez JL, Hendrick MJ, Shofer FS, Goldkamp C, Sorenmo KU. Liposarcomas in dogs: 56 cases (1989–2000). J Am Vet Med Assoc 2004;224:887–891.
19. McEntee MC, Page RL, Mauldin GN, Thrall DE. Results of irradiation of infiltrative lipoma in 13 dogs. Vet Radiol Ultrasound 2000;41:554–556.
20. McEntee MC, Thrall DE. Computed tomographic imaging of infiltrative lipoma in 22 dogs. Vet Radiol Ultrasound 2001;42:221–225.
21. Agut A, Anson A, Navarro A, et al. Imaging diagnosis-infiltrative lipoma causing spinal cord and lumbar nerve root compression in a dog. Vet Radiol Ultrasound 2013;54:381–383.
22. Hammond TN, Regan J. Imaging diagnosis—intra-abdominal necrotic lipoma. Vet Radiol Ultrasound 2008;49:365–367.
23. Tanabe S, Yamada K, Kobayashi Y, et al. Extra-abdominal chondrolipoma in a dog. Vet Radiol Ultrasound 2005;46:306–308.
24. Ben-Amotz R, Ellison GW, Thompson MS, Sheppard BJ, Estrada AH, Levy JK. Pericardial lipoma in a geriatric dog with an incidentally discovered thoracic mass. J Small Anim Pract 2007;48:596–599.
25. Lynch S, Halfacree Z, Desmas I, Cahalan SD, Keenihan EK, Lamb CR. Pulmonary lipoma in a dog. J Small Anim Pract 2013;54:555–558.
26. Kraun MB, Nelson NC, Hollinger C. Imaging diagnosis-computed tomographic, surgical, and histopathologic characteristics of an infiltrative angiolipoma in a dog. Vet Radiol Ultrasound 2015;56:E31–E35.
27. Kitshoff AM, Millward IR, Williams JH, Clift SJ, Kirberger RM. Infiltrative angiolipoma of the parotid salivary gland in a dog. J S Afr Vet Assoc 2010;81:258–261.
28. Hunter JC, Johnston WH, Genant HK. Computed tomography evaluation of fatty tumors of the somatic soft tissues: clinical utility and radiologic-pathologic correlation. Skeletal Radiol 1979;4:79–91.
29. Dooms GC, Hricak H, Sollitto RA, Higgins CB. Lipomatous tumors and tumors with fatty component: MR imaging potential and comparison of MR and CT results. Radiology 1985;157:479–483.
30. Halldorsdottir A, Ekelund L, Rydholm A. CT-diagnosis of lipomatous tumors of the soft tissues. Arch Orthop Trauma Surg 1982;100:211–216.
31. Kransdorf MJ, Moser RP, Jr., Meis JM, Meyer CA. Fat-containing soft-tissue masses of the extremities. Radiographics 1991;11:81–106.
32. Gaskin CM, Helms CA. Lipomas, lipoma variants, and well-differentiated liposarcomas (atypical lipomas): results of MRI evaluations of 126 consecutive fatty masses. AJR Am J Roentgenol 2004;182:733–739.
33. Jelinek JS, Kransdorf MJ, Shmookler BM, Aboulafia AJ, Malawer MM. Liposarcoma of the extremities: MR and CT findings in the histologic subtypes. Radiology 1993;186:455–459.
34. Hosono M, Kobayashi H, Fujimoto R, et al. Septum-like structures in lipoma and liposarcoma: MR imaging and pathologic correlation. Skeletal Radiol 1997;26:150–154.
35. Einarsdottir H, Soderlund V, Larson O, Jenner G, Bauer HC. MR imaging of lipoma and liposarcoma. Acta Radiol 1999;40:64–68.
36. Einarsdottir H, Soderlund V, Larsson O, Mandahl N, Bauer HC. 110 subfascial lipomatous tumors. MR and CT findings versus histopathological diagnosis and cytogenetic analysis. Acta Radiol 1999;40:603–609.
37. Kransdorf MJ, Bancroft LW, Peterson JJ, Murphey MD, Foster WC, Temple HT. Imaging of fatty tumors: distinction of lipoma and well-differentiated liposarcoma. Radiology 2002;224:99–104.
38. Ohguri T, Aoki T, Hisaoka M, et al. Differential diagnosis of benign peripheral lipoma from well-differentiated liposarcoma on MR imaging: is comparison of margins and internal characteristics useful? AJR Am J Roentgenol 2003;180:1689–1694.
39. Murphey MD, Carroll JF, Flemming DJ, Pope TL, Gannon FH, Kransdorf MJ. From the archives of the AFIP: benign musculoskeletal lipomatous lesions. Radiographics 2004;24:1433–1466.
40. Pereira JM, Sirlin CB, Pinto PS, Casola G. CT and MR imaging of extrahepatic fatty masses of the abdomen and pelvis: techniques, diagnosis, differential diagnosis, and pitfalls. Radiographics 2005;25:69–85.
41. Nishida J, Morita T, Ogose A, et al. Imaging characteristics of deep-seated lipomatous tumors: intramuscular lipoma, intermuscular lipoma, and lipoma-like liposarcoma. J Orthop Sci 2007;12:533–541.
42. Lindahl S, Markhede G, Berlin O. Computed tomography of lipomatous and myxoid tumors. Acta Radiol Diagn 1985;26:709–713.

43. Brambilla PG, Roccabianca P, Locatelli C, Di Giancamillo M, Di Marcello M, Pittorru M. Primary cardiac lipoma in a dog. J Vet Intern Med 2006;20:691–693.

44. Case JB, MacPhail CM, Withrow SJ. Anatomic distribution and clinical findings of intermuscular lipomas in 17 dogs (2005–2010). J Am Anim Hosp Assoc 2012;48:245–249.

45. Thomson MJ, Withrow SJ, Dernell WS, Powers BE. Intermuscular lipomas of the thigh region in dogs: 11 cases. J Am Anim Hosp Assoc 1999;35:165–167.

46. Kolm US, Kleiter M, Kosztolich A, Hogler S, Hittmair KM. Benign intrapericardial lipoma in a dog. J Vet Cardiol 2002;4:25–29.

47. Andac N, Baltacioglu F, Cimsit NC, Tuney D, Aktan O. Fat necrosis mimicking liposarcoma in a patient with pelvic lipomatosis. CT findings. Clin Imaging 2003;27:109–111.

48. Varma DG, Muchmore JH, Mizushima A. Computed tomography of infiltrating benign lipoma. J Comput Tomogr 1987;11:45–49.

49. Frazier KS, Herron AJ, Dee JF, Altman NH. Infiltrative lipoma in a canine stifle joint. J Am Anim Hosp Assoc 1993;29:81–83.